Yong Zhao *
Engineering Mechanics Group
Battelle
505 King Avenue
Columbus, OH 43201, USA

Finite Element Modeling and Analysis of Nonlinear Impact and Frictional Motion Responses Including Fluid–Structure Coupling Effects

A nonlinear three dimensional (3D) single rack model and a nonlinear 3D whole pool multi-rack model are developed for the spent fuel storage racks of a nuclear power plant (NPP) to determine impacts and frictional motion responses when subjected to 3D excitations from the supporting building floor. The submerged free standing rack system and surrounding water are coupled due to hydrodynamic fluid–structure interaction (FSI) using potential theory. The models developed have features that allow consideration of geometric and material nonlinearities including (1) the impacts of fuel assemblies to rack cells, a rack to adjacent racks or pool walls, and rack support legs to the pool floor; (2) the hydrodynamic coupling of fuel assemblies with their storing racks, and of a rack with adjacent racks, pool walls, and the pool floor; and (3) the dynamic motion behavior of rocking, twisting, and frictional sliding of rack modules. Using these models 3D nonlinear time history dynamic analyses are performed per the U.S. Nuclear Regulatory Commission (USNRC) criteria. Since few such modeling, analyses, and results using both the 3D single and whole pool multiple rack models are available in the literature, this paper emphasizes description of modeling and analysis techniques using the SOLVIA general purpose nonlinear finite element code. Typical response results with different Coulomb friction coefficients are presented and discussed.

INTRODUCTION

In many operating nuclear power plants spent nuclear fuel assemblies are stored temporarily in stainless steel racks. With many storage cells arranged in a tight array and stored with fuel assemblies, rack modules are heavy structures usually free-standing and submerged in water that is contained in a deep storage pool housed

Received 10 January 1996; Revised 6 May 1997.

*Currently, Sr. Principal Mechanical Modeling Engineer, Medtronic, Inc., Brady Leads Division, 7000 Central Avenue, NE, MS-B248, Minneapolis, MN 55432, USA. E-mail: yong.zhao@medtronic.com

Shock and Vibration, Vol. 4, No. 5,6, pp. 311–325 (1997)
ISSN 1070-9622/97/$8.00

in a building on site. The USNRC has issued overall design requirements and licensing acceptance criteria (USNRC, 1979, 1981) for initial racking activities as well as reracking modifications, in order to increase the temporary storage capacity of a rack from a few hundred fuel assemblies originally designed to several thousand fuel assemblies. After reracking there are usually more than ten high density spent fuel rack modules in existing storage facilities. The overall racking or reracking objective is to maintain subcritically of the spent fuel stored in the close-layout racks under normal and postulated accident conditions and for radiological safety considerations during installation and operation. To this end the racks should be designed such that the structural integrity of both the rack structures and the stored fuel assemblies is assured adequately and the function of the rack modules and storage pool is not lost in normal operation and safe shutdown conditions.

A seismic design or evaluation of spent fuel racks is one of the most important and complicated regulatory requirements. The responses of displacement and impact forces resulting from rack seismic analyses are the first priority parameters for further nuclear criticality, structure, stress, thermal, layout, and other detailed designs and analyses in combination with other load cases.

During postulated strong earthquake motions, the water surrounding racks is accelerated, and hydrodynamic FSI effects are significantly induced between the rack cells and the fuel assemblies, the racks and the pool walls, and the racks with the pool floor (Fritz, 1972; Dong, 1978). Because of the FSI effects, the seismic responses of a submerged structure are usually several times smaller than those of the same structure in air and subject to the same excitations. In the seismic response motions, the free-standing rack support legs may lift off (rock) from, or twist or slide on, the pool floor liner due to inertia effects and friction resistance to the inertia motion of the rack module from the pool floor liner. Such seismic responses of the fluid–structure coupling (FSC) system may cause impacts between rack cells and the fuel assemblies that are free standing inside the rack cells. The impacts of a rack to adjacent racks or the pool walls, and the impacts of rack support legs to the pool floor may also be induced. The mathematical models, usually used to describe such impact and friction phenomena, are materially and geometrically nonlinear. A 3D nonlinear dynamic time history analysis method is needed to solve the nonlinear problems. The USNRC requires that the seismic excitations in the two horizontal directions and the vertical direction must be simultaneously applied. In general, the dimensions of the surrounding gaps, pool, and racks are unsymmetrical in engineering practice.

In postulated seismic events, the significant FSI effects, the materially nonlinear behavior of potential impacts of fuel–rack, rack–rack, rack-pool wall, and rack support–pool floor, and the highly geometrically nonlinear frictional resistance to the motion of the free standing rack supports against the pool floor liner make the nonlinear time history dynamic analysis to be more complicated than for most other nuclear structural systems (Ashar and DeGrassi, 1989; DeGrassi, 1992). An analytical solution for the complicated problems is not available in the literature. A detailed nonlinear dynamic finite element analysis using the hydrodynamically coupled structural elements and fluid elements is computationally impractical. Rather, a simplified finite element analysis with proper modeling and convergent solutions using structural elements plus the FSC effects constitutes an effective numerical approach. However, only limited and simplified experimental verification work is available in the literature.

In most cases, the finite element analysis approaches in the literature are based on the adding hydrodynamic mass concept using potential theory of incompressible and inviscid flow (Fritz, 1972; Dong, 1978; Ashar and DeGrassi, 1989; DeGrassi, 1992). To this end, a finite element analysis is usually performed using the combination of a fuel–rack stick structural model with adding hydrodynamic masses and fluid coupling forces between structures. However, like other complicated engineering problems, the application of the finite element approaches for solving seismic rack evaluation problems is primarily limited by a rational modeling and effective computing effort. Most references available are about analyses using 3D single rack models with uniform gaps (Reed et al., 1979; Sturm and Song, 1980; Durlofsky and Sun, 1981; Harstead et al., 1983) or nonuniform gaps (Scavuzzo et al., 1979; Soler and Singh, 1984; Pop et al., 1990; Singh et al., 1990; Chang, 1994). A 3D single rack model is useful for a detailed analysis and design, but may under predict rack responses due to unsymmetrical FSI effects (DeGrassi, 1992).

Because of the significant FSC effects and directional dependent motion of the racks in a pool, the prediction using a multi-rack model is more rational and accurate than that using a single rack model. However, due to limited modeling techniques and corresponding computing difficulties, only a few analyses were performed using 2D rather than 3D multiple rack models (Kabir et al., 1987; Stabel et al., 1993). It is still difficult for a 2D multi-rack model to simulate rationally the rack motion behavior of sliding, rocking, twisting, and impact, because of the significant 3D FSC effects

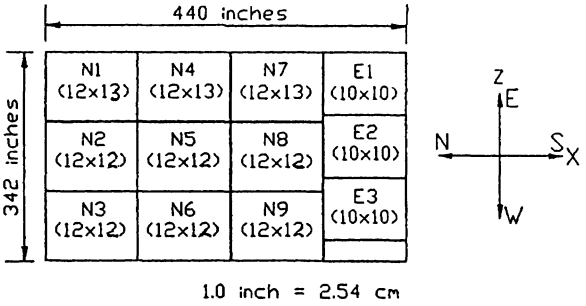

FIGURE 1 Rack layout in a storage pool.

and the potential rocking and twisting motion effects on rack modules.

Few analyses and results using an acceptable 3D whole pool multiple rack model are available in the literature, because such modeling and analysis are much more complicated and computationally difficult than 3D single rack or 2D multi-rack problems. Singh and Soler (1991) reported briefly a 3D whole pool multiple rack analysis using a simplified component element method with a limited number of degrees of freedom (DOF) and its implementing special purpose computer program as discussed by Soler and Singh (1982, 1984). Therefore, for solving rationally the nonlinear seismic evaluation problems of practical rack modules with sufficient accuracy, sophisticated modeling and corresponding analyses using advanced 3D single and whole pool multi-rack models become necessary.

In this paper, the modeling and analysis techniques for a 3D single rack model as well as a 3D whole pool multiple rack model are developed using the general purpose nonlinear finite element code SOLVIA (1992). Prescribed three directional floor seismic motion time histories and the deadweight of rack modules are input simultaneously. Typical results thus obtained for the nonlinear time history dynamic analyses performed with two typical Coulomb friction coefficients (Ashar and DeGrassi, 1989; DeGrassi, 1992) are discussed.

PHYSICAL DESCRIPTION OF FUEL RACK MODULES

Figure 1 shows a typical layout of spent fuel rack modules in a pressurized water reactor (PWR) type NPP. There are nine new racks refereed to as N1 through N9 and three existing racks as E1 through E3. The storage pool is 440 inch (11.18 m) long and 342 inch (8.69 m) wide. The contained water height is about 392 inches (9.96 m). The pool is made of concrete with a steel

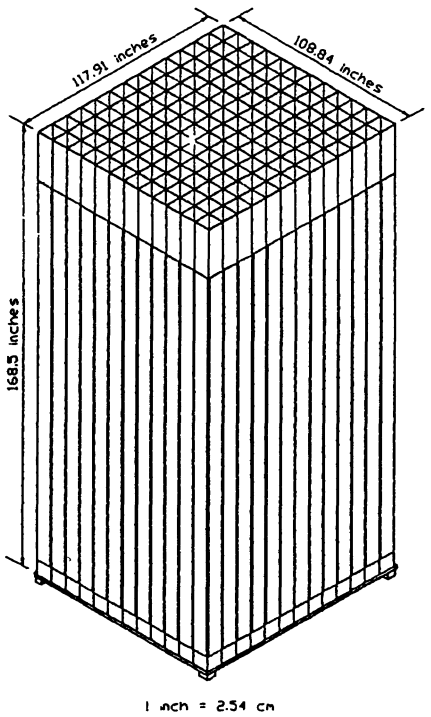

FIGURE 2 Typical 12 × 13 cell rack.

liner on the pool floor and located one a rigid building floor. The building has a fundamental frequency more than 33 Hz.

Figure 2 shows a typical 12 cell by 13 cell (12 × 13) free standing spent fuel storage rack module which is a welded honeycomb stainless steel structure. The spent fuel assemblies stored inside the rack cells are 17 × 17 standard fuel rods. The existing racks are flux type modules with storage cells welded through spacer elements rather than welded directly to adjacent cells at their corners or walls like the honeycomb type modules. The existing racks are 10 × 10 modules. The nominal plane dimensions of the racks and the dimensions of gaps between the racks or between the racks and the pool walls are shown in Table 1.

Each rack cell is designed to store one square-cross-section fuel assembly with a surrounding uniform gap of 0.217 and 0.269 inches (5.15×10^{-3} and 6.83×10^{-3} m) between the fuel assembly surface and the cell walls for the new and existing racks, respectively. The fuel assembly tube is fabricated with thin stainless steel clad. Boral, which is a neutron absorber poison material, is contained in the cell walls. The fuel assemblies are free-standing in the rack cells and the uniform gaps are filled with water.

Along with the storage cells, a rack body also includes other structural members, such as stiffers, top and bottom bumpers, outside boundary flat plates or

Table 1. Dimensions of Racks and Adjacent Gaps (1.0 inch = 2.54 cm)

Dimension (inch)	Rack Module I.D.											
	N1	N2	N3	N4	N5	N6	N7	N8	N9	E1	E2	E3
2B	110.59	110.59	110.59	109.34	109.34	109.34	109.59	109.59	109.59	111.50	111.50	111.50
2C	119.51	109.34	119.51	119.51	109.34	119.51	119.51	109.34	119.51	111.66	111.10	114.10
g_1	2.99	2.99	2.99	0.50	0.50	0.50	0.50	0.50	0.50	1.00	1.00	1.00
g_2	2.70	0.50	0.50	2.70	0.50	0.50	2.70	0.50	0.50	2.70	1.60	1.60
g_3	0.50	0.50	0.50	0.50	0.50	0.50	1.00	1.00	1.00	2.99	2.99	2.99
g_4	0.50	0.50	2.70	0.50	0.50	2.70	0.50	0.50	2.70	1.60	1.60	7.60

bracings, bottom baseplate, and support legs. Each new rack and existing rack has four and seven support legs, respectively. The rack structure is designed so that it can undertake static and dynamic buckling, bending, torsion, and impact type loads in normal operation and accident conditions. The free-standing racks are arranged in the storage pool with gaps between adjacent racks or pool walls. Usually several analyses are needed for racks with different loading conditions of completely or partially filled with fuel assemblies.

When ground seismic excitations are transferred simultaneously in the three orthogonal directions through the housing building to the floor supporting the rack storage pool, the surrounding water in the pool is accelerated and the hydrodynamic FSI effects are induced between the structures of fuel assemblies, racks, and pool walls and floor. The fuel assemblies may rattle, lift-off, and impact cell walls. The free-standing racks may slide, rack, twist and may impact adjacent racks or pool walls and floor liner. The impacts between structures may cause severe local stress or damage and also significantly affect the globe motion behavior of the structures.

3D SINGLE RACK MODEL

Approach and Assumptions

A critical new rack referred to as N7 is chosen for the 3D single rack analyses. Rack N7 with fully stored fuel assemblies weighs about 3.0×10^5 pounds (1.33×10^6 N). As shown in Fig. 3, the 3D single rack stick finite element model is developed using the SOLVIA (1992) code, and is expected to simulate effectively the major physical dynamic response phenomena of sliding, rocking, twisting, and impact. The rack cells are fully loaded with fuel assemblies. The stick model consists of 50 elements (including 28 materially nonlinear impact and geometrically nonlinear contact-friction elements) with a total of 112 degrees of freedom (DOF) and 13 1D rigid links.

As shown in the pool layout in Fig. 1, Rack N7 is surrounded by other two new racks N4 (12 × 13) and N8 (12 × 12) with a gap of 0.5″ (0.013 m), respectively, and existing rack E1 (10 × 10) with a gap of 1.0″ (0.025 m), and the pool wall with a gap of 2.99″ (0.076 m). Rack N7 will be modeled appropriately using stick structural finite elements with features simulating the major motion behavior described in previous sections for both the rack structure and fuel assemblies stored. The 3D single rack model developed herein is based on the following basic assumptions:

1. The water is incompressible and inviscid or frictionless, i.e., potential theory is effective and Lagrange's equations of motion can be applied. Fluid damping is small and neglected. These assumptions were verified with sufficiently accurate tests for engineering purposes and are acceptable to the regulatory requirements (Fritz, 1972; Dong, 1978; USNRC, 1979, 1981; Ashar and DeGrassi, 1989; DeGrassi, 1992);
2. The fuel assemblies are conservatively assumed to move in phase so that they can be modeled using a single fuel bundle or stick. The fuel bundle is free standing at the center of the rack structure that is also represented using a single stick. This assumption is conservative for determining a maximum fuel–rack impact;
3. Rack N7 is simply assumed to move in phase with adjacent racks so as to use the initial physical gap dimensions between the racks and pool walls. This assumption is appropriate especially when no or small rack–rack impacts occur, since the FSC effects intend to move the racks together;
4. The FSC effects between racks or pool walls are considered only for adjacent racks or pool walls, so that rack N7 can be isolated for developing a 3D single rack model (Pop et al., 1990).

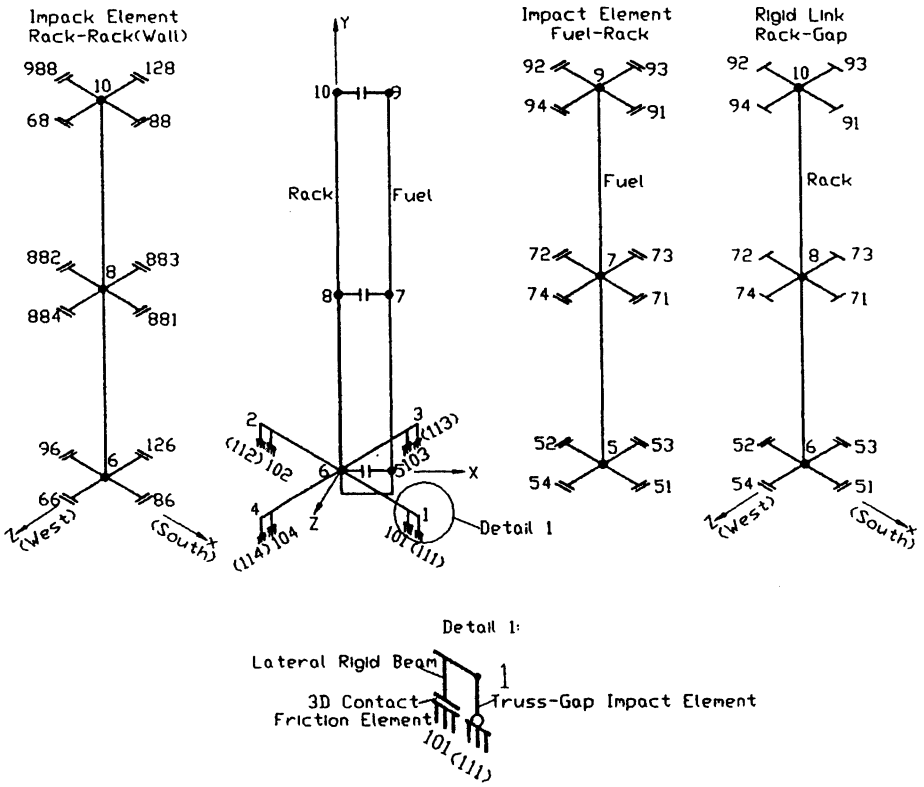

FIGURE 3 3D single rack stick finite element model.

Fluid–Structure Interaction Effects

The FSI effects can be rationally taken into account using the hydrodynamic mass concept based on potential theory and Lagrange's equations of motion (Fritz, 1972; Dong, 1978), which has been used widely in the literature and accepted and recommended by the US-NRC (1979, 1981). The adding hydrodynamic mass approach allows use of available structural analysis finite element codes and stick finite element stick models. Based on the analytical, numerical, and experimental work by Fritz (1972), Dong (1978), Scavuzzo et al. (1979), Pop et al. (1990), and Singh et al. (1990), for two submerged rectangular cylinders with four non-uniform gaps filled with water as shown in Fig. 4, the hydrodynamic mass M_{Hx} due to relative motion in the horizontal X direction is extended numerically herein as

$$M_{Hx} = 2\rho hC^2(C/3g_1+C/3g_3+B/g_2+B/g_4), \quad (1)$$

in which ρ is the water mass density, h is the cylinder height, C and B are the nominal dimensions, and g_1, g_2, g_3, and g_4 denote gap sizes around. Similarly, the hydrodynamic mass M_{Hz} due to relative motion in the horizontal Z direction can also be determined.

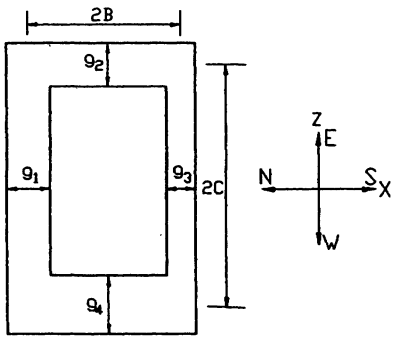

FIGURE 4 Cross section dimensions of two rectangular cylinders coupled by fluid.

From Eq. (1) it is noted that the smaller the gap sizes are, the larger the hydrodynamic mass will be. The motion of larger size solid structures coupled with fluid causes larger hydrodynamic masses. The hydrodynamic masses may be many times larger than the solid masses of structures. It should be pointed out that Eq. (1) needs to be verified further using sophisticated physical tests or numerical calculation with a combination of coupling fluid elements and solid structural elements.

Using Eq. (1) it is noted that the hydrodynamic masses M_{Hx} and M_{Hz} calculated separately in the two horizontal directions are usually not identical, since the surrounding gap sizes are unsymmetrical in practice. The effects due to the variation of the gap sizes on the hydrodynamic masses during seismic-induced motion are not large until the gap on one side becomes very small (Singh et al., 1990), and, therefore, are not taken into account herein.

The hydrodynamic coupling between any two solid masses, Mass 1 representing a fuel assembly mass and Mass 2 a rack mass, is then described as 'adding' forces due to the relative motion of the two masses in the X direction using the following equation of motion:

$$\begin{vmatrix} F_{x1} \\ F_{x2} \end{vmatrix} = \begin{vmatrix} M_1 + M_2 + M_{Hx} & -(M_1 + M_{Hx}) \\ -(M_1 + M_{Hx}) & M_{Hx} \end{vmatrix} \times \begin{vmatrix} \ddot{X}_1 \\ \ddot{X}_2 \end{vmatrix}, \quad (2)$$

where F_{x1} is the adding force acted on Mass 1, F_{x2} the adding force acted on Mass 2 which is assumed be contained inside Mass 1, M_1 the mass of water displaced by Mass 2, M_2 the mass of water enclosed by Mass 1 in the absence of Mass 2, M_{Hx} the hydrodynamic mass, and $\ddot{X}_1$, $\ddot{X}_2$ the absolute accelerations of Mass 1, Mass 2.

Equation (2) means that larger hydrodynamic masses cause larger adding forces acting on the coupled solid structures. When the water masses M_1 and M_2, and the hydrodynamic masses M_{Hx} and M_{Hz} are computed separately in the two orthogonal horizontal directions for each coupled solid mass pair, the mass matrix in Eq. (2) for the adding masses (diagonal terms) and the hydrodynamic coupling effects (off-diagonal terms) between any coupled solid Mass 1 and Mass 2 are easy to calculate and add to the structural analysis purpose finite element stick model, as shown in Fig. 3 by use of a full size general mass matrix element for the whole model. This approach can be used for the hydrodynamic coupling considerations between the fuel bundle and the rack as well as between the rack and adjacent racks or pool walls.

The vertical hydrodynamic coupling in the Y direction between the rack baseplate and the pool floor may also be considered similarly using the hydrodynamic mass M_{Hy} determined by (Fritz, 1972)

$$M_{Hy} = K(\pi\rho a^2 b/4), \quad (3)$$

in which, $K = 0.487$, a and b are the dimensions of the baseplate, and ρ is water mass density. The M_{Hy} value calculated usually is many times less than the value of M_{Hx} or M_{Hz}.

Fuel Assemblies

As shown in Fig. 3, all the fuel assemblies are modeled as a single bundle. The fuel bundle is represented using two 3D massless beam elements. The mass of the fuel bundle is lumped in the three directions to the bottom, middle, and top of the bundle. The lateral and vertical stiffness of the beams are provided primarily by the clad of the fuel assemblies rather than the fuel rods, since the fuel rods are installed inside the fuel assemblies and are not required to resist external mechanical loading by the initial designs.

The fuel–rack impact at the three fuel mass locations in the North, South, West, and East directions is modeled using twelve materially nonlinear 1D truss–gap impact elements with initial physical gaps of $0.217''$ (5.51×10^{-3} m). Twelve 1D displacement type rigid links are needed to work with the twelve impact elements, since only one directional impact is active at any instant when the impact occurs.

The impact stiffness of the fuel bundle to the rack body with N rack cells is determined by

$$K = NK_i, \quad (4)$$

$$1/K_i = 1/K_{ir} + 1/K_{if}, \quad (5)$$

where K_i is the ith fuel–rack impact stiffness consisting of the ith rack cell stiffness K_{ir} and the ith fuel assembly fitting spring stiffness K_{if}. The parameter K_{ir} is calculated using a beam model fixed at both ends subjected to a concentrated load at the center of the beam,

$$K_{ir} = 192EI_i/L^3, \quad (6)$$

in which I_i is the moment of inertia of the ith rack cell with the width dimension of L. E is the modulus of elasticity of the rack steel.

Based on the assumption that the fuel bundle is free-standing and remains vertical contact with the rack at the fuel bundle bottom, a vertical constraint is specified between the rack body and the fuel bundle at the bottom of the fuel bundle. This assumption is made due to the limitations of a general purpose finite element code for a substructure that is not allowed to include contact–friction elements. The effects due to the assumption are estimated to be minor, because the fuel bundles are usually about ten times heavier than the rack body and the vertical excitation is only two thirds of the horizontal one. However, this needs to be verified in the future.

Rack Structure

In Fig. 3 the rack body is modeled as two 3D massless beam elements and three lumped 3D mass elements

at the bottom, middle, and top of the rack body. The rack stick is located at the geometrical center of the rack body. The beam and mass elements are defined with the horizontal and vertical stiffness values determined from the rack cells and other related structural members. The rack mass at the bottom also includes those lumped from the rack baseplate and support legs. Because of its relative stiffer properties than the rack body, the rack baseplate is modeled using four rigid massless 3D beams connecting at one end with four support legs at their physical locations and at the other end with the bottom rack mass. The purpose of using the physical plane locations of the support legs is to simulate effectively the potential rocking and twisting motion behavior of the rack structure.

Four geometrically nonlinear 3D contact–friction elements are define to model the motion behavior of the vertical contact and the horizontal frictional sliding at the interfaces of the support legs and the pool floor liner. The physical gaps at the interfaces are initially closed. A support leg lifts off and then the friction resistance to this leg is inactive when its associated gap is open during motion. The pool floor with a steel liner is a part of the building, the floor is assumed to be rigid and serves as the target contact surfaces for the 3D contact–friction elements.

The rack support legs are modeled as four massless 3D beam elements with their calculated vertical axial composite stiffness to transfer the vertical excitation and with the rigid lateral stiffness to transfer the horizontal excitations from the bottom of the rack supports to the rack body. The compression stiffness K_s of each rack support consists of a series of the local vertical floor stiffness K_f, the leg axial stiffness K_l, and the baseplate local stiffness K_p, and can be calculated by

$$1/K_s = 1/K_f + 1/K_l + 1/K_p. \tag{7}$$

Four materially nonlinear 1D truss–gap impact elements are defined for simulating the potential vertical impacts between the rack support legs and the pool floor liner, when the initially closed physical gaps are opened and closed and back and forth, or the so-called rack tilting or rocking phenomenon occurs.

The fuel–rack impact modeling has been described in the previous section about the fuel assemblies. Another group of twelve 1D materially nonlinear truss–gap impact elements between the rack and adjacent racks or pool walls are defined in the four horizontal directions at the three rack mass locations, which will be active only when the corresponding rack displacement responses are larger than the physical gap dimensions in the same directions.

The rack–rack impact stiffness may be determined approximately using test-based engineering experience data or from references. The rack–pool wall impact stiffness can be computed approximately and conservatively using the numerical formulas and parameters given by Timoshenko and Woinowsky-Krieger (1959) through the model of a vertical concrete wall with three edges fixed subject to uniform fluid pressure. It is noted that such rack–rack and rack–pool wall impact stiffness values are only optional and do not affect the desired rack response results if there is no such impact occurring. However, a comprehensive analysis of the rack–rack and rack–pool wall impact is needed if the impacts occur.

Friction Effects

The friction effects on a pair of relatively moving and contacting solid bodies are complicated phenomena that depend on study philosophies used and many internal and external factors, such as material properties of the bodies, roughness of the sliding interfaces, lubricant properties between the interfaces, static or dynamic motion status, relative motion speed, environment temperature and pressure. A detailed investigation of the complicated frictional phenomena and effects exceeds the objective of this paper for a particular engineering problem.

Nevertheless, the USNRC (1979, 1981) recommended and accepted the Coulomb static friction coefficient of 0.2 as a lower bound and 0.8 as an upper bound to describe the sliding friction resistance of the pool floor liner to the lateral motion of the bottom surfaces of the rack support legs. This range was determined statistically by Rabinowicz (1976) from his 199 stainless steel rack sliding test results including the effects of surface finishes and sliding speed. Therefore, the constant static friction coefficients of 0.2 and 0.8 are used herein separately to evaluate the effects of the friction coefficients on the dynamic responses of rack N7. The values of the Coulomb friction coefficient used to describe the friction resistance essentially govern the motion behavior of the free standing rack.

Damping Effects

Damping effects of fluid due to the FSI effects are small and can be neglected (Dong, 1978; USNRC, 1979, 1981). The damping considered in the 3D single rack model is from the rack module structure only. Rayleigh damping (Clough and Penzien, 1975) is appropriate for a nonlinear dynamic time history analysis. Rayleigh damping, which is proportional to mass as well as stiffness, is defined as

$$[C] = \alpha[M] + \beta[K], \tag{8}$$

where $[C]$ is the Rayleigh damping matrix, $[M]$ is the mass matrix except the hydrodynamically added mass, $[K]$ is the stiffness matrix, α and β are constants determined by

$$\xi_i = \alpha/(4\pi f_i) + \beta\pi f_i, \tag{9}$$

in which ξ is the viscous damping ratio, f is frequency, and i is the index of a frequency value. Using the prescribed critical viscous damping of 3.0% in a frequency range of 5.0 to 25.0 Hz in this case, the values of the parameters α and β can be computed. It is noted that, for Rayleigh damping, forcing the viscous damping to 3.0% at 5.0 and 25.0 Hz conservatively gives somewhat lower and conservative viscous damping values than 3.0% between 5.0 and 25.0 HZ.

3D WHOLE POOL MULTI-RACK MODEL

In engineering practice since detailed nonlinear time history analyses are usually conducted first for design purposes using 3D single rack models, the primary objective of a nonlinear dynamic time history analysis using a 3D whole pool multi-rack model is to investigate the response behavior for all rack modules stored in a pool, and to verify whether there are rack–rack or rack–pool wall impacts.

A 3D whole pool multiple spent fuel storage rack model developed herein is shown in Fig. 5. The model includes the nine new racks and three existing racks (Fig. 1). In contrast to the three lumped rack and fuel mass pairs located at the top, middle, and bottom of the rack body in the 3D single rack model described previously in Fig. 3, there are only two lumped rack and fuel mass pairs at the rack top and bottom in the 3D whole pool model so as to reduce the total number of DOF and the associated expensive computing effort, which constitutes the major difference of the finite element mesh between the single rack model and the whole pool multi-rack model.

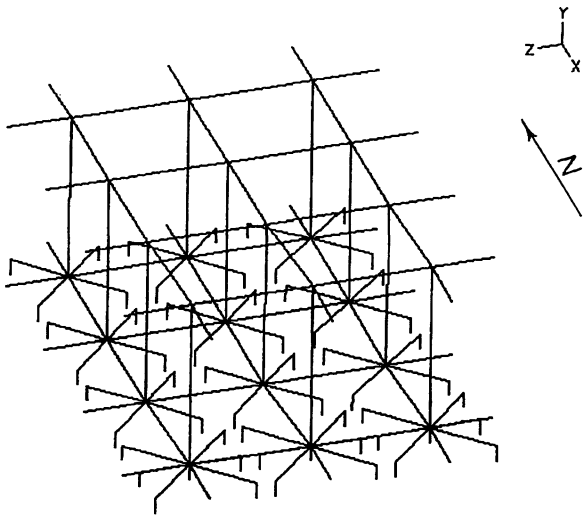

FIGURE 5 Whole pool multi-rack finite element model.

In the whole pool multi-rack model, each new rack module is modeled with two lumped 3D mass elements connected by one massless 3D beam element for the rack body and fuel bundle separately, eight materially nonlinear rack–fuel impact truss–gap elements and associated eight 1D rigid links, one 1D vertical rigid link for the rack and fuel masses at the rack bottom, four rigid massless 3D beam elements for the baseplate, four geometrically nonlinear 3D contact–friction elements, four massless 3D beam and four 1D truss–gap impact elements for the support legs, and eight 1D truss–gap impact elements for the potential rack–rack and rack–pool wall impacts.

There are a total of 42 elements (including 20 nonlinear impact and contact–friction elements) with a total of 96 DOF and nine 1D rigid links for a stick model of the nine new rack modules. Each of the three existing racks has seven support legs which are exactly modeled. The existing racks are modeled using a similar stick model as for the new rack modules. However, an existing rack stick model developed has two more baseplate beam elements, three more 3D support contact–friction elements, three more support leg beam elements, and three more leg–pool floor impact truss–gap elements than the new rack stick model, which brings a total of 53 elements (including 21 nonlinear impact and contact–friction elements) with 138 DOF and nine 1D rigid links.

In summary, after taking out the common impact elements and rigid links counted duplicately between racks, the 3D whole pool multiple rack model developed herein consists of a total of 537 elements (including 263 nonlinear impact and contact–friction elements) with 1278 DOF and 108 1D rigid links, which can simulate the dynamic response behavior of sliding, rocking, twisting, and impact for the 12 rack modules. All the new and existing rack modules and fuel bundles, surrounding water, and pool walls are hydrodynamically coupled in the whole pool model.

The hydrodynamic masses for each mass pair of fuel–rack, rack–rack, and rack–pool wall are determined separately using Eq. (1) with the physical gap sizes. The adding hydrodynamic coupling force approach for the hydrodynamic mass matrix expressed in Eq. (2) can be used for each solid mass pair and then a general mass matrix is assembled for the whole multiple rack structure model. The vertical hydrodynamic

coupling in the Y direction between the rack baseplate and pool floor liner for each rack module is also computed using the method described in the development of the single rack model. The impact stiffness values for the fuel–rack, rack–rack, and rack–pool wall impact are determined one by one using the same procedures as those used for the single rack model.

It should be noted that the 3D whole pool multirack model developed in this case is relatively large for a complicated nonlinear time history dynamic analysis, and special computing effort must be needed to assure desirable responses of interest.

3D NONLINEAR DYNAMIC TIME HISTORY ANALYSES

The Coulomb friction coefficients of 0.2 and 0.8 are used separately to perform nonlinear dynamic time history seismic response analyses with the 3D single rack model. Based upon the response results obtained in the single rack model analyses, one friction coefficient value corresponding to a severe displacement response condition will be determined to perform a 3D whole pool multiple rack nonlinear time history dynamic analysis to verify potential rack–rack or rack–pool wall impact phenomena.

The uncorrelated 3D seismic excitations are the prescribed specific floor motion time histories of acceleration with a peak floor horizontal acceleration of $0.2g$ for a safe shutdown earthquake (SSE) event (Fig. 6). The floor excitation time histories are applied simultaneously in the three orthogonal directions plus the vertical deadweight of the rack modules. The vertical excitation peak values is two thirds of the horizontal ones. The seismic excitation duration of 20 s is fully considered in the 3D single rack analyses. However, the analysis using the 3D whole pool multiple rack model is cut off at about 14 s which covers all the maximum responses observed in the single rack analyses due to storage limitations and excessive computation for the relatively larger 3D whole pool model.

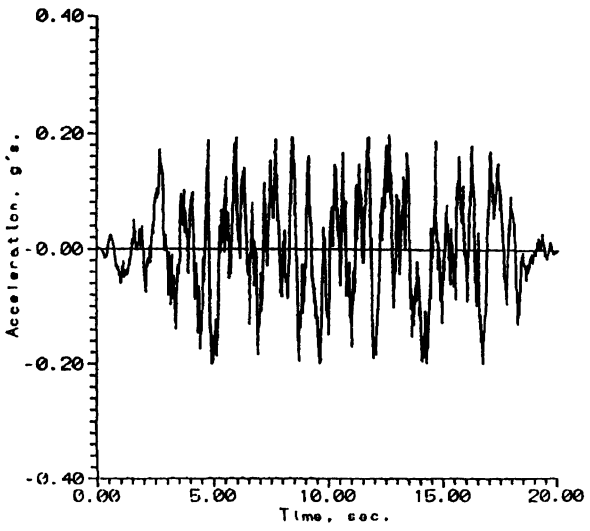

FIGURE 6 Floor acceleration response time history in the N–S direction.

It is extremely important to use a sufficient small time step in a nonlinear time history dynamic analysis, especially when using the 3D whole pool multirack model, with contact–friction elements in order to achieve stable and convergent response results. After several tests, a time step of 0.0015 s is optimized in the nonlinear dynamic analyses for a good convergence with an acceptable iteration speed and with a small number of iterations.

When performing the nonlinear time history dynamic analyses, the Newmark direct time integration method is employed. The Full–Newton iteration scheme with energy and displacement convergence criteria is specified. An elastic–perfectly-plastic material mode is defined for the stainless steel impact elements. The responses obtained using the combination of the numerical techniques specified in this study is quite stable and convergent for the complicated large 3D nonlinear time history dynamic calculations.

The general purpose nonlinear finite element code SOLVIA (1992) is employed for the nonlinear 3D dynamic time history analyses. SOLVIA has been commercial about six years and was developed from the ADINA code which has been used widely and successfully in the nuclear industry for nonlinear problems for more than 16 years.

RESULTS AND DISCUSSIONS

Typical seismic response results of the 3D single rack module N7 (Figs. 1 and 2) are shown in Fig. 7 when the friction coefficient is equal to 0.8. The results indicate that the rack deflection is small but dominates the rack motion behavior, since the displacement at the rack top is relatively larger than that at the rack bottom. The maximum rack displacement of $0.017''$ (4.32×10^{-4} m) is found in the N–S direction at the instant of about 16 s. It is noted that the smaller gaps and relative smaller stiffness (only 12 rather than 13 cells) are found in that direction. No tilting or uplift occurs since the vertical displacements of the supports are near zero at a few instants. The fuel bundle behaves like a rigid body moving inside the rack cell in horizontal directions. However, it impacts the rack cell sometimes since its displacements

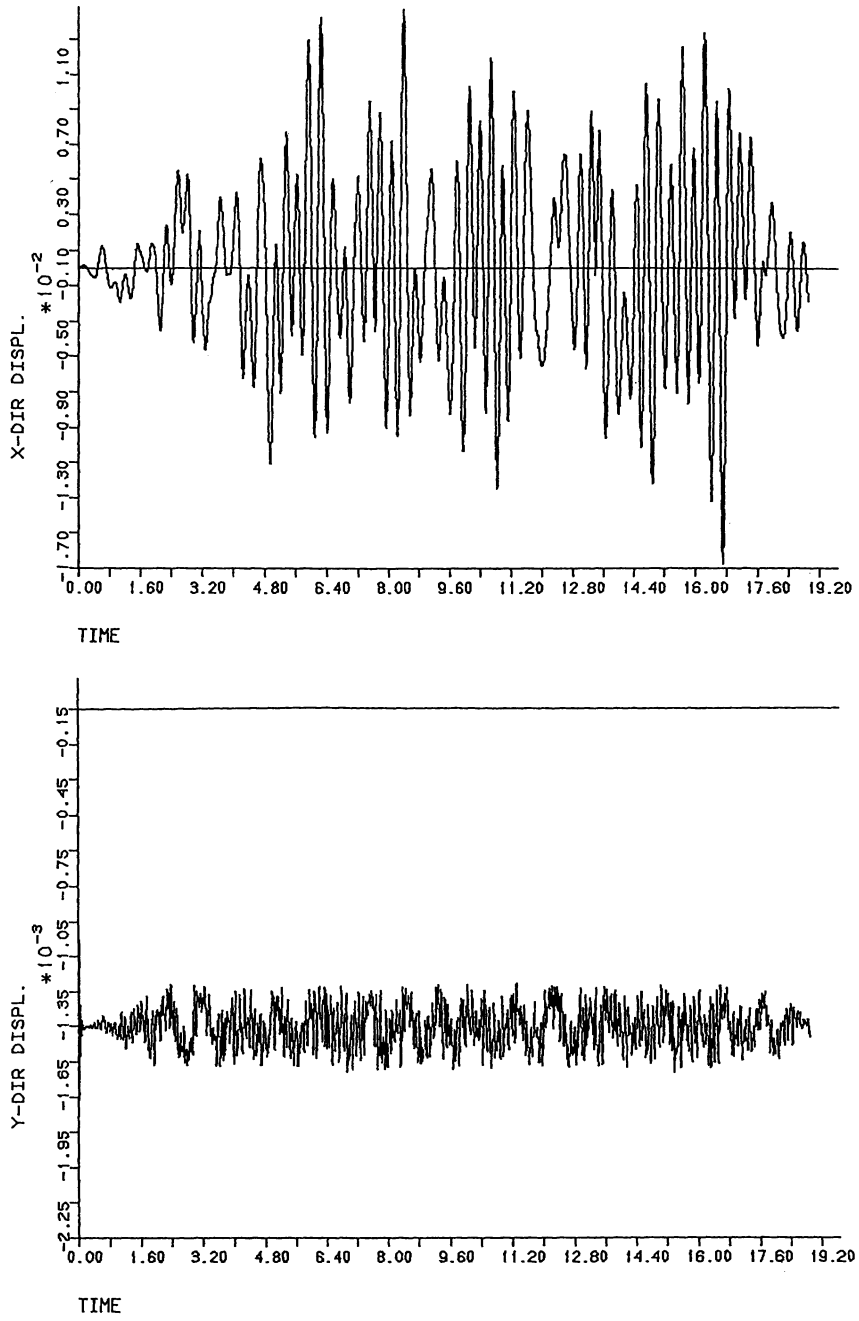

FIGURE 7 Typical responses of rack N7 using 3D single rack model with the friction coefficient equal to 0.8. (a) Rack top displacement in the N–S direction. (b) Rack top displacement in the vertical direction.

are greater than the surrounding uniform physical gaps of 0.217″ (5.51×10^{-3} m). The fuel–rack impacts occur at all three elevations with a maximum value of 1282 pounds (5702 N) per cell at the rack top in the North direction. Detailed line type fuel–rack impact stress analysis is needed and possible on the basis of the maximum impact force value obtained in this study. There is no rack–rack or rack–pool wall impact occurring with rack N7 because the maximum rack displacements are always less than the physical gap dimensions listed in Table 1 and shown in Figs. 1 and 4.

Figure 8 shows some response results of the 3D single rack module N7 in the case of the friction coefficient equal to 0.2. The results demonstrate that sliding dominates the rack motion behavior, because the differences between the rack top and bottom displace-

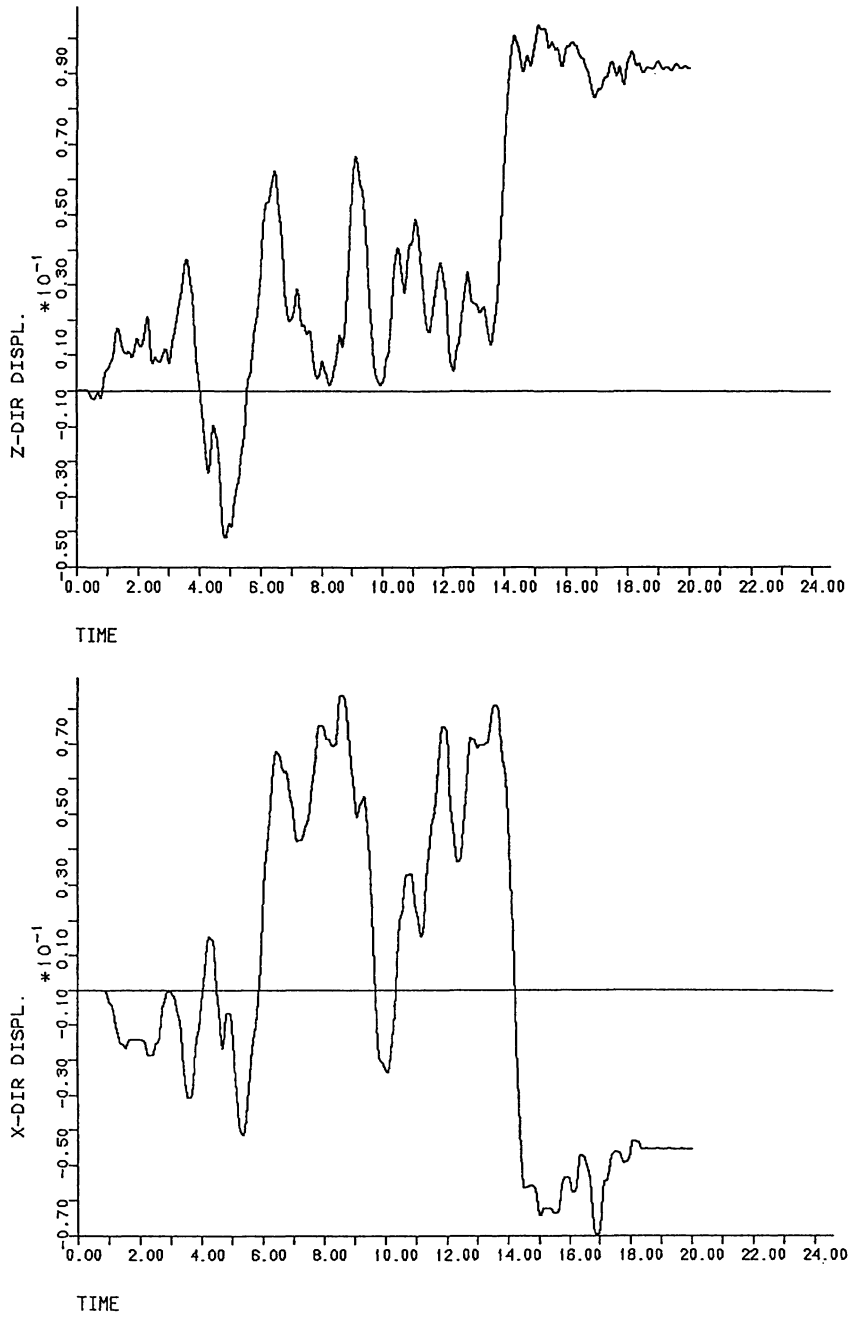

FIGURE 8 Typical responses of rack N7 using 3D single rack model with the friction coefficient equal to 0.2. (a) Rack top displacement in the E–W direction. (b) Rack bottom displacement in the N–S direction.

ments are much smaller than the displacement values. The maximum displacements at the rack top in the N–S and E–W directions are separately about 5 and 14 times those obtained when the friction coefficient is equal to 0.8. The largest rack displacement is 0.103″ (2.62×10^{-3} m) in the E–W direction occurring about 14 s after the motion direction is changed from the North ($+X$) direction to the South ($-X$) direction. It is noted that the largest displacement range at the rack top is still in the N–S direction due to the larger hydrodynamic FSI effects existing in that direction.

The comparisons of the displacement response time histories of rack N7 in the cases of the friction coefficients equal to 0.8 and 0.2 demonstrate that the variation of the friction coefficient significantly affects not only the value but also the direction of the displace-

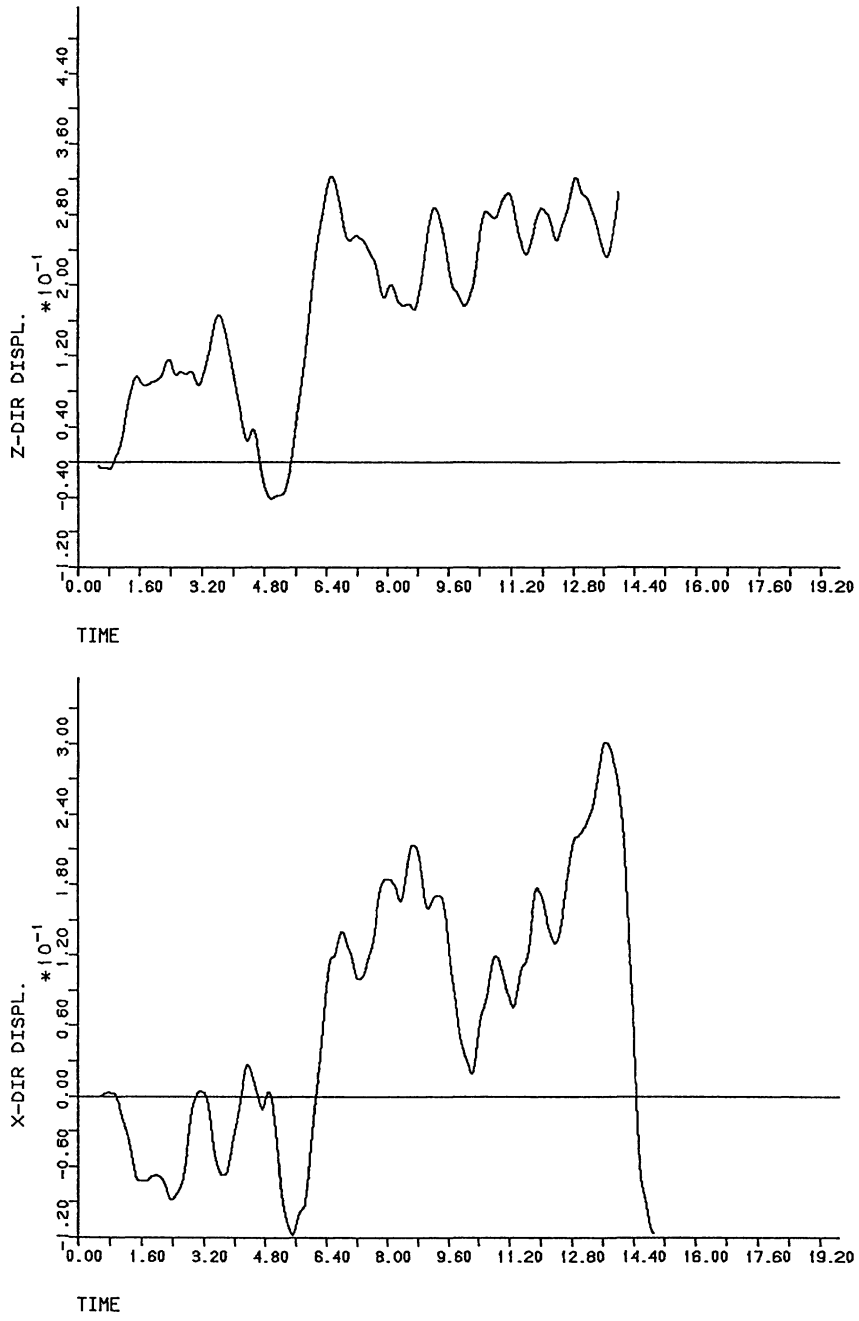

FIGURE 9 Typical responses of rack N7 using 3D whole pool model with the friction coefficient equal to 0.2. (a) Rack top displacement in the E–W direction. (b) Rack bottom displacement in the N–S direction.

ment responses which are loading history dependent. With the strong friction effects the largest displacement in an absolute sense may happen in the direction with relatively weaker FSI effects like this typical case, when the difference of the hydrodynamic effects in the two directions is not large, and when the excitations in the two directions have the same peak values but are statistically independent.

From the results obtained it is found that no rocking occurs, since the vertical displacements at the four rack supports are nearly zero and the negative or compression contact forces remain unchanged in sign. The fuel–rack impacts take place sometimes only in the N–S direction with a maximum impact force of 523 pounds (2326 N) per cell, which is about five times smaller than that obtained when the coefficient of fric-

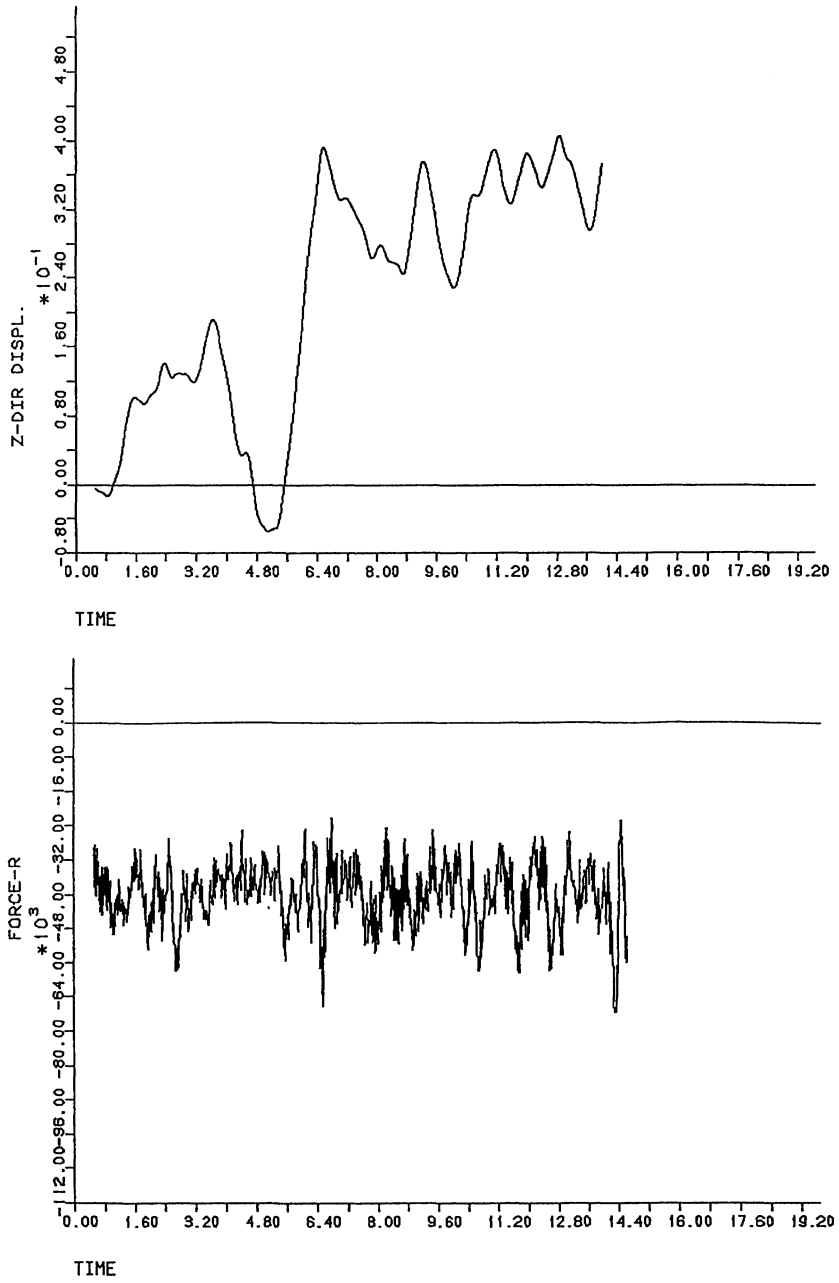

FIGURE 10 Typical responses of rack N4 using 3D whole pool model with the friction coefficient equal to 0.2. (a) Rack top displacement in the E–W direction. (b) Contact force on the S–E support surface.

tion is equal to 0.8. This means that the higher the coefficient of friction is, the larger the fuel–rack impact force will be, because the friction resistance basically acts on the rack legs, while the fuel bundle is free standing inside the rack cell and has the same inertial motion that is not affected by the friction resistance for the same prescribed excitations. No rack–rack or rack–pool wall impact is found, since the maximum rack displacements are also less than the surrounding physical gap sizes and the corresponding impact forces from the associated impact elements are always equal to zero.

The responses obtained from the 3D single rack analyses demonstrate that the rack structure is sufficiently stiff to resist bending, torsion, and shear type loads. The stick with three lumped masses and two beams can effectively represent the rack body and the fuel bundle with sufficient accuracy.

It is found that the responses obtained in this 3D single rack study are in general consistent with those by most researchers in the literature. The 3D single rack model developed is thus verified to be effective and, therefore, can be extended to develop the 3D whole pool multi-rack model.

The coefficient of friction of 0.2 is found to be the upper bound for the rack displacement responses in the 3D single rack analysis (Fig. 8). Therefore, it is used for the 3D whole pool multiple rack model analysis. Partial response results obtained are presented in Figs. 9 and 10 for typical rack modules N7 and N4.

The displacements at the top of rack N7 (Fig. 9) are found to be about 2.8 (in the N–S direction) to 3.2 (in the E–W direction) times those computed in the single rack model analyses with a coefficient of friction equal to 0.2, which means that the 3D single rack model may underpredict the responses by about three times in this case. The relative larger displacement increment in the E–W direction may be due to the stronger hydrodynamic FSC effects in this direction from the adjacent racks N8, N4, and E1.

Of all the 12 rack modules the worst seismic responses are found with rack N4 (Fig. 10). Rack N4, like rack N7, is a 12×13 cell module, however, its gaps of 0.5″ (0.013 m) in the East with rack N1, West with rack N7, and South with rack N5, and its gap of 2.99″ (0.076 m) in the North with the pool wall, are equal to or smaller than those surrounding rack N7 as described previously. Therefore, its motion is affected stronger by the larger adding hydrodynamic masses and fluid coupling forces, and exhibits higher displacement responses than rack N7. For rack N4, the higher hydrodynamic coupling effects and with 12 cells more in the E–W direction than in the N–S direction may be the reason for the largest displacement of 0.41″ (0.010 m) in the E–W direction. The negative contact forces of the support legs of rack N4 indicate that no tilting or uplift occurs. The fuel–rack impacts occur only at a few time points with a maximum value of 897 pounds (3990 N) per cell, which is less than that obtained in the single rack analysis.

Of the three existing rack modules, rack E2 exhibits the largest displacement responses which are about 3.5 times lower than those of rack N4. It is noted that there is no fuel–rack impact found for the existing racks. Rack E2 does not tilt or uplift since its support legs keep in contact with the pool floor. The major reason for the relative smaller responses of the existing racks, in contrast to the new rack modules, lies in the fact that the larger gaps between the fuel assemblies and the rack cell walls, the larger gaps between the racks and the pool walls, and the smaller nominal rack dimensions may cause smaller adding hydrodynamic masses and coupling forces. On the other hand, because of more structural members, the existing racks are 1.6 times heavier and up to 1.8 times stiffer than the new racks N7 and N4.

No rack–rack or rack–pool wall impact is found for all the twelve rack modules, because the rack displacements are less than the surrounding physical gap dimensions, and the corresponding impact forces from the associated impact elements are always equal to zero.

It should be noted that, on the basis of simple tests and verification studies for single rack models as described previously, the approach developed for and the results obtained from the 3D whole pool multi-rack model in this study are implicit, and need further verification using sophisticated tests and numerical analyses.

CONCLUDING REMARKS

The modeling and the seismic evaluation are completed using the 3D single rack model and the 3D whole pool multiple rack model developed independently for the specific case. The 3D nonlinear dynamic time history analyses are performed according to the USNRC requirements. The hydrodynamic FSI effects and potential impacts of fuel–rack, rack–rack, and rack–pool wall are taken into account. Coulomb coefficients of friction of 0.2 and 0.8 are used in the single rack analyses and 0.2 in the whole pool multiple rack analysis. Some observations in this specific study are: (1) the modeling techniques of using the stick structural model based on the concept of adding hydrodynamic masses and fluid coupling forces are effective for developing the 3D single rack model, and can be extended to the 3D whole pool multi-rack model for practical engineering problems; (2) the fuel–rack impact exists at a few instants in the new racks but not in the existing racks, the higher the coefficient of friction is, the larger the fuel–rack impact forces but the lower rack displacement responses will be. The maximum fuel–rack impact force is determined from the 3D single rack analysis with a friction coefficient of 0.8; (3) no rack–rack, or rack–rack walls, or rack–pool floor impact occurs; (4) the frictional sliding governs the motion of the free standing racks without tilting or uplift; (5) the 3D single rack analyses under predict the displacement responses of the rack modules by about three times those obtained in the 3D whole pool multiple rack model analysis, that can be used for determine the maximum rack displacements; (6) larger responses happen in the direction with stronger hydrodynamic coupling effects; and (7) the observations through this

study provide essential information for further detailed designs and analyses of nuclear criticality, structure, stress, thermal, and layout in combination with other load cases.

REFERENCES

Ashar, H., and DeGrassi, G., 1989, "Design and Analysis of Free-Standing Spent Fuel Racks in Nuclear Power Plants (An Overview)," *SMiRT* 10, K2, pp. 595–600.

Chang, S. J., 1994, "Seismic Anlysis of Submerged Spent Fuel Storage Structure," *ASME PVP*, Vol. 271, pp. 73–82.

Clough, R. W., and Penzien, J., 1975, *Dynamics of Structures*, 2nd ed., McGraw-Hill, Inc.

DeGrassi, G., 1992, "Review of the Technical Basis and Verification of Current Analysis Methods Used to Predict Seismic Reponse of Spent Fuel Storage Racks," NUREG/CR-5912, October.

Dong, R. G., 1978, "Effective Mass and Damping of Submerged Structures," UCRL-52342, Lawrence Livermore Laboratory, April.

Durlofsky, H., and Sun, P. C., 1981, "Fuel/Module Impact Load in a Submerged Fuel Storage," *SMiRT* 6, August, J8/9.

Fritz, R. J., 1972, "The Effects of Liquids on the Dynamic Motions of Immersed Solids," *Journal of Engineering for Industry, Trans. ASME*, pp. 167–173, February.

Harstead, G. A., et al., 1983, "Seismic Analysis of High Density Spent Fuel Storage Racks," ASME 83-NE-11.

Kabir, A. F., et al., 1987, "Nonlinear Analysis of Spent-Fuel Racks for Consolidated Fuel Loading," *SMiRT* 9, August, Vol. K1, pp. 409–414.

Pop, J. Jr., Putman, S. F., and Singh, S., 1990, "Nonlinear Dynamic Analysis of Spent Fuel Storage Racks," *ASME PVP*, Vol. 191, pp. 113–118.

Reed, J. W., Webster, F. A., and Sun, P. C., 1979, "Alternative Structural Systems for High Density Fuel Storage Racks in Existing Facilities," *SMiRT* 5, August, K4/4.

Rabinowicz, E., 1976, "Friction Coefficients of Water-Lubricated Stainless Steel for a Spent Fuel Racj Facility," Massachusetts Institute of Technology, November.

Scavuzzo, R. J., Stokey, W. F., and Ragke, E. F., 1979, "Dynamic Fluid–Structure Coupling of Rectangular Modules in Rectangular Pools," *ASME PVP*, Vol. 39, June, pp. 25–29.

Singh, K. P., and Soler, A. I., 1991, "Chin Shan Analyses Show Advantages of Whole Pool Multi-Rack Approach," *Nuclear Engineering International*, March, pp. 37–40.

Singh, S., Putman, S. F., and Pop, J. Jr., 1990, "Structural Evaluation of Onsite Spent Fuel Storage: Recent Developments, Curent Issues Related to Nuclear Power Plant Structures, Equipment and Piping," *Proceedings of the Third Symposium, Orlando, Florida*, December, pp. V/4 1–18.

Soler, A. I., and Singh, K. P., 1982, "Dynamic Coupling in a Closely Spaced Two-Body System Vibrating in a Liquid Medium: the Case of Fuel Racks," *The 3rd Keswick International Conference – Vibration in Nuclear Plants*, Keswick, U.K., May.

Soler, A. I., and Singh, K. P., 1984, "Seismic Response of a Free Standing Fuel Rack Construction to 3D Floor Motion," *Nuclear Engineering and Design*, Vol. 80, pp. 315–329.

SOLVIA Engineering AB, 1992, *Users Manual for SOLVIA*, Revision 90.2, April.

Stabel, J., Ren, M., and Swelim, H., 1993, "Calculation of Seismic Loads on Fuel Storage Racks under Consideration of Fluid–Structure Interaction," *SMiRT* 12, August, K15/6, pp. 61–66.

Sturm, A. J. Jr., and Song, C. S., 1980, "The Effects of Submergence on Structural Response in Confined Pools," *Nuclear Engineering and Design*, Vol. 60, pp. 287–296.

Timoshenko, S., and Woinowsky-Krieger, S., 1959, "Theory of Plates and Shells," 2nd ed., McGraw-Hill, Inc.

USNRC, 1979, "OT Position for Review and Acceptance of Spent Fuel Storage and Handling Applications," January, modification to this document of April 1978.

USNRC, 1981, NUREG-0800, Standard Review Plan, Section 3.8.4, Appendix D, "Technical Position on Spent Fuel Pool Racks."